Undirected graphical model of adjacency matrix for dynamic elasticity in polyelectrolyte hydrogels

Ziyu Xing[a], Dong-Wei Shu[b], Haibao Lu[a,*] and Yong-Qing Fu[c]

[a]National Key Laboratory of Science and Technology on Advanced Composites in Special Environments, Harbin Institute of Technology, Harbin 150080, China

[b]School of Mechanical and Aerospace Engineering, Nanyang Technological University, 50 Nanyang Avenue, 639798, Singapore

[c]Faculty of Engineering and Environment, University of Northumbria, Newcastle upon Tyne, NE1 8ST, UK

[*]Corresponding author, E-mail: luhb@hit.edu.cn

Abstract: Molecular network plays a critical role in determining dynamic elasticity of soft condensed polymers, e.g., their varied cross-linking densities and end-to-end distances with changed Young's moduli. Although it has been studied for decades, the coupling relationship between vertices and edges of molecular networks is not well understood, mainly because the degree of the crosslinking points and asymmetry molecular networks have not been considered in the previously models. In this study, a graph theory was employed to formulate an undirected graphical model and describe the coupling between vertices and edges in molecular networks, based on which the dynamic elasticity of polyelectrolyte hydrogel was modeled. From the Kirchhoff graph theory and bead-spring model, the coupling relationship between vertices and edges was obtained using end-to-end distance and viscosity parameters. Combining the Watts–Strogatz model and kinetic probability, the coupling between vertices and

edges for the polyelectrolyte network was studied. Furthermore, an adjacency matrix with eigenvalue, number of vertices and mean degree was proposed to formulate constitutive relationships including dynamic elasticity and stress-strain, according to rubber elasticity theory and Mooney-Rivlin model, respectively. The linking between the vertices and edges determines the network structure and dynamic elasticity of the polyelectrolyte hydrogel. Based on the graph theory, the vertices and edges are encoded by adjacency matrix, which is proposed to describe the dynamic elasticity of symmetric and asymmetric network structures using the crosslinking density and end-to-end distance. Finally, effectiveness of the undirected graphical model was verified using both finite element analysis and experimental results of polyelectrolyte hydrogels reported in literature.

Keywords: Graph theory; polyelectrolyte; dynamic elasticity; adjacency matrix

1. Introduction

Soft matters have shown various fascinating mechanical behaviors, such as stiffening-adaptive chameleon skin, bending-adaptive sunflower stalk, folding-induced Venus flytrap, and twisting-responsive seed pod [1-8]. Therefore, a great number of studies have been conducted to study the mechanics of these soft matters [9-11]. Among them, hydrogels are the most attractive soft matters owing to their ultra-high stretchability and nonlinear stress-strain behaviors [13]. However, the poor strength and toughness do limit their practical applications. To improve the mechanical performance, ionic bonds have often been introduced into hydrogels (e.g., forming polyelectrolyte ones) [14-17], which have been explored for applications in

batteries [14], electronics [15] and sensors [16,17].

So far, the constitutive relationship between molecular network structures and dynamic elasticity of these polyelectrolyte hydrogels is largely unknown, although there are some previous reports on this topic [18-27], including the rubber elasticity theory based on the knot theory [18], 8-chain model [19], viscoelasticity models [20,21], and statistical conformation models [22-25]. Unfortunately, these models can not well explain the constitutive relationship between crosslinking points (or vertices in geometry) and end-to-end distances (or edges in geometry) in these molecular networks, thus resulting in a large divergence between analytical results obtained using these proposed models and the experimental data [26-30]. For example, in the previously reported classical models [18-25], elasticity of molecular networks has been formulated using the constitutive relationship between number of crosslinking points and the end-to-end distances. However, the parameters applied in these phenomenological models were mainly determined by the experimental results, and the coupling effects among them have not been well considered and explored. Previously, the coupling effect between crosslinking points (or vertices in geometry) and end-to-end distances (or edges in geometry) has been described using the graph theory [28-30], which provides a probability approach to formulate the loading transfer and describe the dynamic elasticity using the adjacency matrix of vertices and edges. Therefore, new methods, such as those based on the graph theory [28-30] could be applied to describe the constitutive and coupling relationship between vertices and edges for the molecular network, of which the dynamic elasticity plays an essential

role to determine the mechanical behavior of these types of polymers.

In this study, an undirected graphical model has been formulated to explore the coupling between vertices and edges and characterize the molecular networks using end-to-end distance and viscosity parameters, based on the bead-spring model [26,27] and Kirchhoff graph theory [31-32]. Then the proposed model is extended to describe the polyelectrolyte network based on the Watts–Strogatz model, by combining the dynamic probability with external loadings and their mechano-chemical coupling [33-35]. Furthermore, an adjacency matrix with eigenvalue, number of vertices and mean degree has been developed to formulate constitutive relationships such as dynamic elasticity and stress-strain relationship, according to the rubber elasticity theory and Mooney-Rivlin model, respectively [36-39]. Finally, effectiveness of this newly proposed model is verified using both finite element analysis (FEA) and experimental results of polyelectrolyte hydrogels reported in literature [21,40-42]. This study is expected to provide a fundamental approach to formulate the constitutive relationship between vertices and edges of symmetric molecular networks, of which the dynamic elasticity is described and predicted using the adjacency matrix of undirected graph model.

2. Theoretical framework

For molecular network in polymers, an adjacency matrix (**A**) can be written to describe the mechanics between vertices and edges, based on the graph theory [28-30],

$$\mathbf{A} = \begin{cases} 1 & \text{if vertices } v_i \text{ and } v_j \text{ are bonded} \\ 0 & \text{otherwise} \end{cases} \tag{1}$$

where v_i and v_j are vertexes (crosslink points in a molecular network), i and j are integer counter from 1 to N, N is the number of vertices in the molecular network and order for adjacency matrix ($\mathbf{A}_{N\times N}$). The matrix coding of the network structure are shown in Figure 1(a). The terminology in graph theory and polymer science are mutually exchangeable [26-35] as listed in Table 1, where all the other important parameters will be introduced in this section.

Table 1. Comparison between the terminologies in graph theory and in polymer physics [26-35].

Terminology in graph theory	Terminology in polymer physics
Graph	Network structure
Adjacency matrix (**A**)	Rouse matrix (2**I**-**A**) in bead-spring model
Vertices	Crosslink points
Edge	Chain
The order of **A** or vertex number (N)	The number of crosslink points
Degree (d_i)	Functionality of crosslink points
Mean degree (d)	The average of functionality
Eigenvalue (Λ_i)	Relaxation time spectrum

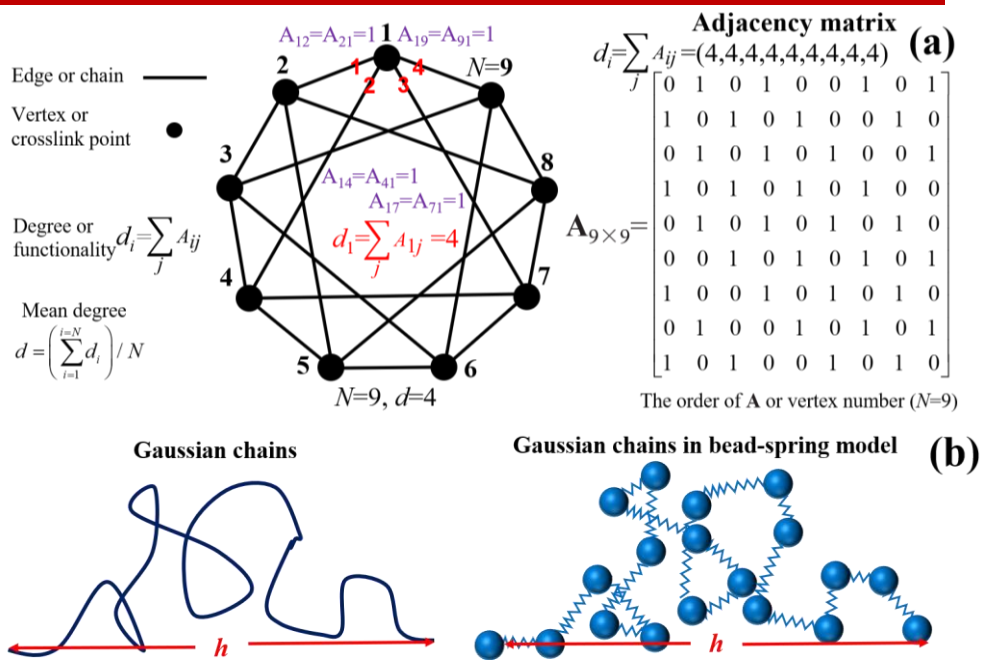

Figure 1. (a) Matrix coding of the network structure of polymer based on graph theory. (b) The configuration properties of Gaussian chains based on the bead-spring model

According to the bead-spring model [26,27], the eigenvalue of adjacency matrix (Λ_{li}) of the linear chain matrix (2**I-A**) is written as,

$$\Lambda_{li} = 4\sin^2\left[\frac{i\pi}{2(N+1)}\right] \tag{2}$$

where 2**I-A** is the Rouse matrix to describe viscoelastic and configurational properties of Gaussian chains based on the bead-spring model [26,27], as described in Figure 1(b). **I** is the unit matrix with diagonal elements of 1.

Based on equation (2), the relaxation time (τ_l), viscosity (η_l), and end-to-end distance (h_l) of linear polymer chains can be obtained [26],

$$\tau_{li} = \frac{h_s^2}{2b^2\xi\Lambda_{li}} \tag{3a}$$

$$\eta_l = N_{el}k_BT\sum_{i=1}^{N}\tau_{li} = \frac{N_{el}k_BTh_s^2}{2b^2\xi}\sum_{i=1}^{N}\Lambda_{li}^{-1} \tag{3b}$$

$$h_l^2 = \frac{h_s^2}{N}\sum_{i=1}^{N}\Lambda_{li}^{-1} \tag{3c}$$

where h_s is end-to-end distance of a segment, b is the length of a molecule in the segment, ξ is the relative velocity of bead-spring, N_{el} is the number of elastic chains, k_B=1.38×10^{-23} J/K is the Boltzmann constant and T is the temperature.

For a polyelectrolyte hydrogel, the reactions among the charged polymer chains follow a probability manner. An extended Kirchhoff graph theory [31,32] is often used to describe the end-to-end distances in terms of eigenvalues for the 2**I-A**,

$$\frac{h_b^2}{h_l^2} = \frac{\sum_{i=1}^{N}\Lambda_{bi}^{-1}}{\sum_{i=1}^{N}\Lambda_{li}^{-1}} = \frac{3d-2}{d^2} \tag{4}$$

where h_b is the end-to-end distance for branched chains, and d is the mean degree of

the number of crosslink points.

In the Affine network, the degree of a v_i vertex is defined as the number of edges connected to the v_i vertex as then shown as d_i [39]. The sum of all entries on the i th row of **A** is $\sum_j A_{ij}$, and the sum of all entries on its i-th column is $\sum_j A_{ji}$. In a molecular compound, the number of bonds is defined as the functionality of crosslink points [28-30].

Meanwhile, the probability ($P(d_i)$) of molecular networks follows the Poisson distribution function, based on the Watts–Strogatz model [33-35],

$$P(d_i = \sum_j A_{ij}) = \frac{\exp(-d)d^{d_i}}{d_i!} \tag{5}$$

The reactions among the charged polymer chains follow the probabilistic mode of the Poisson distribution [33-35]. The extent of reaction is governed by the chemical reaction kinetics, which is mainly determined by the initial and final concentrations of the charged polymer chains in the polyelectrolyte hydrogel [38].

In the polyelectrolyte hydrogel, there are a lot of free charged chains that cannot be involved in the molecular networks. Therefore, the eigenvalue of matrix (2**I**-**A**) of the polyelectrolyte hydrogels can be rewritten as,

$$\frac{\sum_{i=1}^{N}\Lambda_i^{-1}}{\sum_{i=1}^{N}\Lambda_{li}^{-1}} = \frac{1}{N}\sum_{i=1}^{N}\frac{3d_i-2}{d_i^2}\frac{\exp(-d)d^{d_i}}{d_i!} \approx \frac{3d-2}{d^2}\frac{d^d}{e^d d!} \tag{6}$$

where Λ_i is the eigenvalue of matrix (2**I**-**A**) for the polyelectrolyte hydrogel.

Combining equations (3) and (6), where the assumptions of combination of equations (3) and (6) have been presented in the Section of S1 in the Supporting

Materials, the viscosity (η) and end-to-end distance (h) of the polyelectrolyte hydrogel are obtained, as follows,

$$\eta = \frac{N_{el} k_B T h_s^2}{2b^2 \xi} \sum_{i=1}^{N} \Lambda_{li}^{-1} \frac{3d-2}{e^d d!d^{2-d}} \tag{7}$$

$$h^2 = \frac{h_s^2}{N} \sum_{i=1}^{N} \Lambda_{li}^{-1} \frac{3d-2}{e^d d!d^{2-d}} \tag{8}$$

where the definition of the end-to-end distance (h) of the polyelectrolyte hydrogel has been presented in the Section of S2 in the Supporting Materials.

Moreover, according to the rubber elasticity theory [36-39], the elastic free energy (ΔF_{el}) of molecular network can be expressed as,

$$\Delta F_{el} = -\frac{N_{el} k_B T}{2} J_m \ln(1 - \frac{I_1 - 3}{J_m}) \tag{9}$$

$$I_1 = \lambda_1^2 + \lambda_2^2 + \lambda_3^2 = \lambda^2 + \frac{2}{\lambda} \tag{10}$$

where λ_1, λ_2 and λ_3 represent the stretching ratios along three directions of the molecular networks, respectively. The relationships of $\lambda_1=\lambda$ and $\lambda_2=\lambda_3=\lambda^{-1/2}$ are used in the uniaxial tensile stretching of molecular networks (in which λ is the elongation ratio), assuming the volume invariance of isotropic material, i.e., $\lambda_1\lambda_2\lambda_3=1$. $J_m \propto h^2/h_s^2$ is the ultimate tensile strength based on the Gent model [36,37].

According to the Kelvin model [38] and Mooney-Rivlin model [39], the modulus of molecular networks can be written as $N_{el}k_BT(1+\dot{\lambda}\eta/\lambda)$, under a uniaxial tension loading. Based on these, a constitutive relationship of stress (σ) as a function of elongation ratio can be obtained as,

$$\sigma = \frac{\partial \Delta F_{el}}{\partial \lambda} = \frac{(1+\frac{\dot{\lambda}}{\lambda}\frac{h_s^2}{2b^2\xi}\sum_{i=1}^{N}\Lambda_i^{-1})N_{el}k_BT(\lambda-\frac{1}{\lambda^2})}{1-\frac{N(\lambda^2+2/\lambda-3)}{J_m\sum_{i=1}^{N}\Lambda_i^{-1}}} \tag{11a}$$

$$\frac{\sum_{i=1}^{N}\Lambda_i^{-1}}{\sum_{i=1}^{N}\Lambda_{li}^{-1}} = \frac{1}{N}\sum_{i=1}^{N}\frac{3d_i-2}{d_i^2}\frac{\exp(-d)d^{d_i}}{d_i!} \approx \frac{3d-2}{d^2}\frac{d^d}{e^d d!} \tag{11b}$$

where $\dot{\lambda}$ is strain rate. Here all the different types of networks follow the Affine network assumptions.

Different from the classical graph theory which does not consider the distribution of degrees [28-30], as shown in equations (1), (2), (3), (4), (5) and (9), our newly proposed model (as shown in equations (6), (7), (8), (10) and (11)) not only encodes the network into the adjacency matrix, but also considers the distribution of degrees. It can handle complex networks (e.g., the asymmetric graphical networks).

To verify the above proposed model based on equation (11), the analytical results of stresses as a function of elongation ratio for the polyelectrolyte hydrogel have been plotted, in which the graph network is governed by equation (11). The parameters used in equation (11) for calculations of these values are N=8, $N_{el}k_BT$=0.1 MPa, J_m=800 and $\frac{h_s^2\dot{\lambda}}{2b^2\xi}$=1. The number of vertices (N) is used as the number of the crosslink points. Figure 2 shows the constitutive stress-elongation ratio relationship which has been obtained with the mean degrees (d) of 2, 3, 4, 5, 6 and 7. With an increase in the mean degree (d) from 2, 3, 4, 5, 6 to 7, the stress of graph network is gradually increased from 1.44 MPa, 1.46 MPa, 1.62 MPa, 2.04 MPa, 2.98 MPa to

5.50 MPa at the same elongation ratio of λ=8.2. These analytical results indicate that the mean degree (d), which quantifies the interaction between vertices and edges, plays an essential role in determining the elasticity of the graph network. This is mainly attributed to the increased functionality of crosslink point in the molecular networks based on the rubber elastic theory [39].

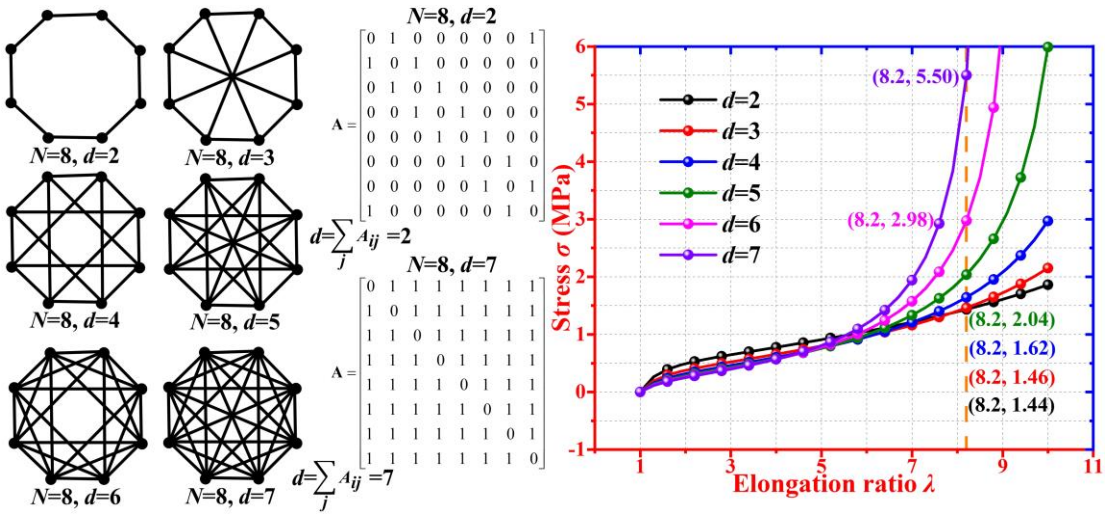

Figure 2. Constitutive stress-elongation ratio curves for the polyelectrolyte hydrogel, of which the graph network is determined by the mean degree of d=2, d=3, d=4, d=5, d=6 and d=7, at the same vertex number of N =8 in molecular network.

Analytical results of effects of vertex number (N, which is used to characterize the order in adjacency matrix as $\mathbf{A}_{N\times N}$) on stress-elongation ratio were further obtained based on equation (11) and the obtained results are plotted in Figure 3. Parameters used in equation (11) for calculations of these values are d=4, $N_{el}k_BT$=0.1 MPa, J_m=800 and $\frac{h_s^2\dot{\lambda}}{2b^2\xi}$ =3. With an increase in the vertex number (N) from 5, 6, 7, 8 to 9, the stress of graph network is gradually increased from 1.53 MPa, 1.54 MPa, 1.58 MPa, 1.66 MPa to 1.75 MPa at the same elongation ratio of λ=7. These analytical results indicate that the vertex number (N) plays an essential role in determining the

dynamic elasticity of the graph network. This is mainly attributed to the increased end-to-end distance (h) for molecular network, resulted from the increased vertex number (N) in the graph network based on the bead-spring model [26] and rubber elastic theory [39]. Based on these results, we can see that the graph network is able to present a sphere structure with an increase in the vertex number (N), where the mean degree (d) is kept a constant, thus resulting in an increased end-to-end distance (h) of the networks.

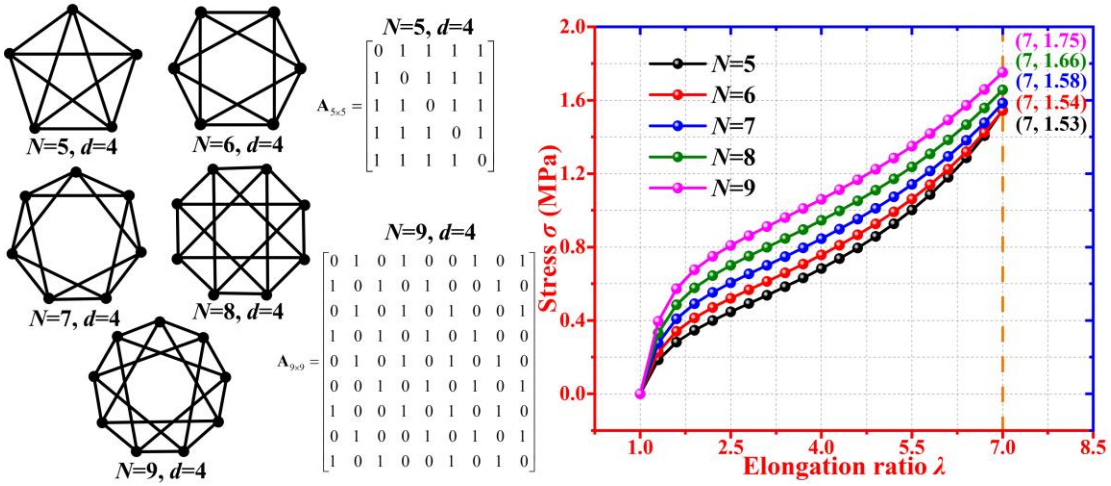

Figure 3. Constitutive stress-elongation ratio curves for the polyelectrolyte hydrogel, of which the graphical network is determined by the vertex number of N=5, N=6, N=7, N=8 and N=9, at the same mean degree (d=4) in molecular network.

On the other hand, the order (N) in the adjacency matrix $\mathbf{A}_{N\times N}$ can reflect the dynamic elasticity of graphical network. For example, the adjacency matrix $\mathbf{A}_{9\times 9}$ reveals that there are nine crosslinking points in the network to resist the external loading, and the dynamic elasticity is better than those with the lesser five crosslinking points with adjacency matrix $\mathbf{A}_{5\times 5}$ [26-30].

It should be noted that the above-mentioned study was carried out for the undirected graphical network using the adjacency matrix, which were often used to

characterize the directed and asymmetric graphical networks. Effects of asymmetry of directed graphical networks on stress-elongation ratios were further investigated using equation (11) and the results are plotted in Figure 4, at the same given values of vertex number N=6 and mean degree of d=1.67. Parameters used in equation (11) for calculating these values are $N_{el}k_BT$=0.1 MPa, J_m=480 and $\frac{h_s^2\dot{\lambda}}{2b^2\xi}$=6.

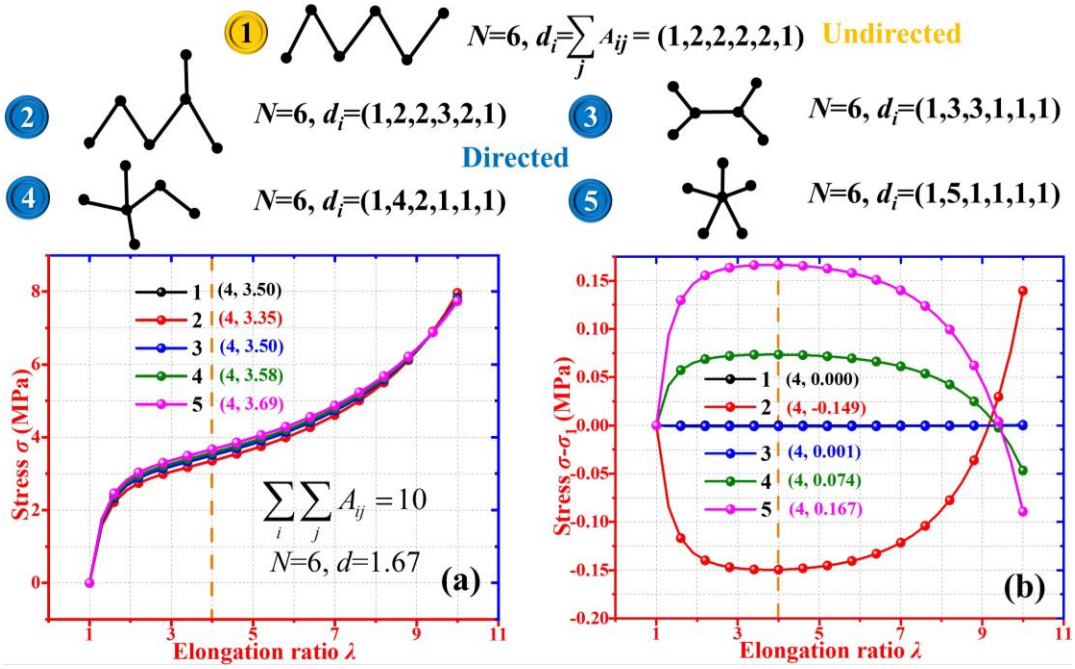

Figure 4. Constitutive stress-elongation ratio curves for the polyelectrolyte hydrogel with the undirected and directed graph networks at the same vertex number of N=6 and mean degree of d=1.67. (a) For the stress-elongation ratio curves. (b) Divergences of undirected and directed graph networks of the stress as a function of elongation ratio.

The obtained stresses of directed graphical networks are 3.35 MPa, 3.50 MPa, 3.58 MPa and 3.69 MPa, in comparison with that of undirected graph network of 3.50 MPa, at the same elongation ratio of λ=4, as shown in Figure 4(a). Meanwhile, the divergences between the undirected (d_i=(1,2,2,2,2,1)) and directed (d_i=(1,2,2,3,2,1), d_i=(1,3,3,1,1,1), d_i=(1,4,2,1,1,1) and d_i=(1,5,1,1,1,1)) graphical networks were calculated using equation (11), and the obtained data are -0.149 MPa, 0.001 MPa,

0.074 MPa and 0.167 MPa, respectively, as shown in Figure 4(b). These analytical results reveal that the dynamic elasticity of the molecular network is critically affected by its symmetry and asymmetry, which can be characterized by the mean degree (d) to describe the order of the edges.

3. Finite-element analysis (FEA) and experimental verification

3.1 FEA simulation

A commercial software (ABAQUS, 3DS Dassault Systems, France) was used for finite-element analysis (FEA). We used the FEA to characterize the effects of vertex number (N) and mean degree (d) on the constitutive stress-strain relationships of the undirected graphical networks, and the obtained results are shown in Figure 5. The Young's modulus and Poisson's ratio of the edges of molecular networks were chosen as 1 MPa and 0.45 [39], respectively, in the simulations. The 2-node beam element, B31, was used to perform the calculation, and 1000 elements were used to model the whole unit. The area of the closed polygon is 500 mm^2, and the section of beam is a circle with a radius of 0.2 mm. The polyelectrolyte network structure in the FEA model is about 10^6 times larger than that in the molecular network of the hydrogel.

The obtained FEA results of stress-strain (σ-ε) are plotted for the undirected graphical network with the mean degrees (d) of 2, 3, 4, 5 and 6, at a given vertex number of N=8, as shown in Figure 5(a). It is revealed that the stress of undirected graphical network is gradually increased from 0.02 MPa, 0.38 MPa, 0.46 MPa, 0.47 MPa to 0.50 MPa at the same strain of ε=0.4, with an increase in the mean degrees (d) from 2, 3, 4, 5 to 6.

On the other hand, the FEA results of stress-strain (σ-ε) results are plotted for the undirected graphical network with the vertex numbers (N) of 5, 6, 7, 8 and 9, at a given mean degree of d=4, as shown in Figure 5(b). These simulation results present that the stress of undirected graph network is gradually increased from 0.40 MPa, 0.43 MPa, 0.45 MPa, 0.46 MPa to 0.52 MPa with an increase in the vertex number (N) from 5, 6, 7, 8 to 9, at the same strain of ε=0.4. These FEA results broadly support that the mechanical property and elasticity of molecular network can be improved by the increase in vertex number (N) or mean degree (d).

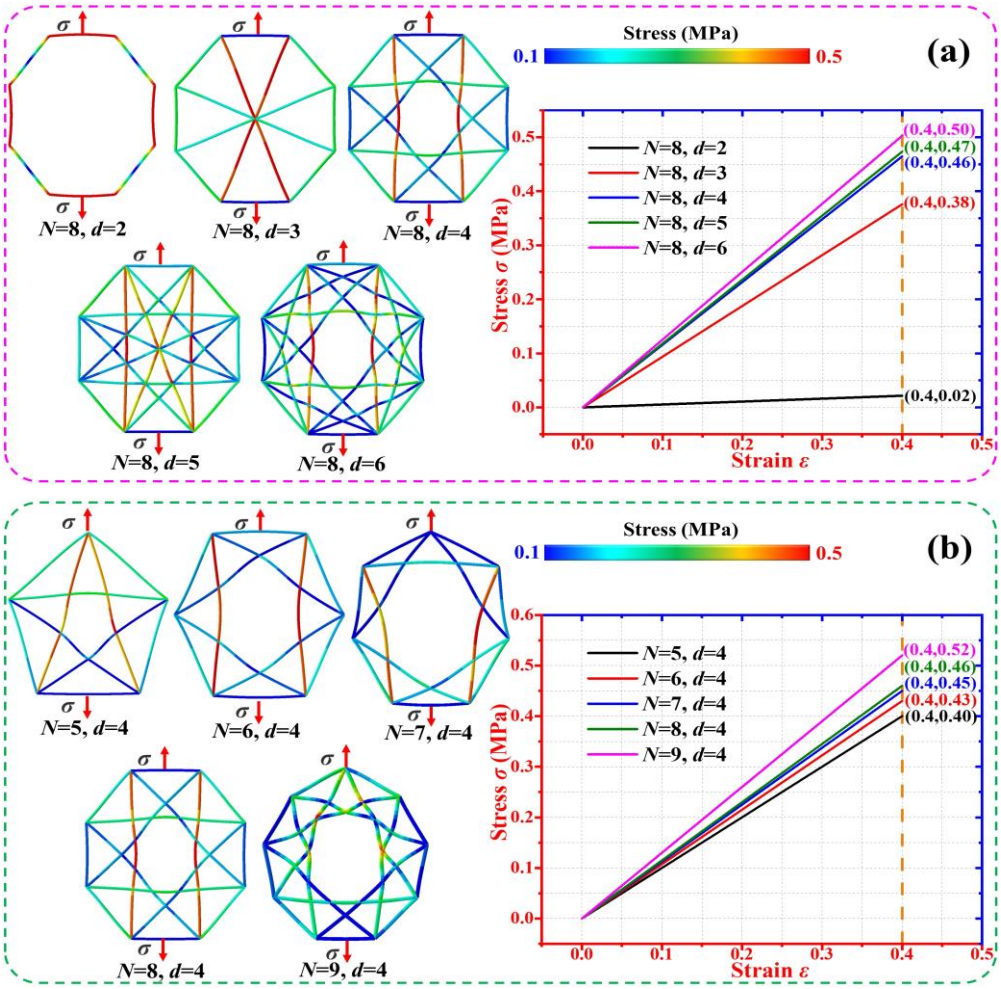

Figure 5. Effects of vertex number (N) and mean degree (d) on the constitutive stress-strain relationship of the undirected graph network, based on the FEA simulations. (a) Effect of mean degree (d). (b) Effects of vertex number (N).

3.2 Experimental verification

Five groups of experimental data [21,40-42] of polyelectrolyte hydrogels were collected to verify the analytical results generated from the proposed model of equation (11). Here, $N_{el}k_BT$ is linked to the modulus of polyelectrolyte hydrogel based on the rubber elasticity theory [36-39], N_{el} is the number of elastic chains in polyelectrolyte hydrogel, k_B=1.38×10^{-23} J/K is the Boltzmann constant, T≈298.15 K is the temperature and J_m is the material constant [36-37]. Λ_i is the eigenvalue of matrix (2**I**-**A**) [26,27,31,32] for polyelectrolyte hydrogels, 10<N<100 is the order in $\mathbf{A}_{N\times N}$ adjacency matrix [27,39], 2<d<6 is the mean degree (or functionality of crosslink point) in $\mathbf{A}_{N\times N}$ adjacency matrix [27,39]. $\dot{\lambda}$ is the strain rate ranged from 0.007 s^{-1} to 1.25 s^{-1} reported in Ref. [21,40-42], h_s is the end-to-end distance of a segment, b is the length of segment, ξ= 1 s^{-1} is the relative velocity of bead-spring [26] and $\frac{h_s^2\dot{\lambda}}{2b^2\xi}$ is ranged from 0.0035 to 0.625. The Levenberg-Marquardt optimization algorithm was adopted for all the calculation parameters.

Table 2. Values of parameters used in equation (11) for PAAc and PAAm polyelectrolyte hydrogels.

	$N_{el}k_BT$(kPa)	N	d	J_m	$\frac{h_s^2\dot{\lambda}}{2b^2\xi}$
PAAc	1.32	62	4	1200	0.1
PAAm	2.86	47			

To verify the proposed model of equation (11), the obtained analytical results have been plotted in Figure 6(a) to predict the stress-elongation ratio behavior of the PAAc (polyacrylic acid) and PAAm (polyacrylamide) polyelectrolyte hydrogel [40]. All the parameters used in the calculation using equation (11) are listed in Table 2. Figure

6(b) shows the correlation index R^2 between the analytical and experimental results, which are 99.21% and 99.79% for PAAc and PAAm polyelectrolyte hydrogels, respectively. It can be clearly seen that the proposed model well predicts the mechanical properties of the PAAc and PAAm polyelectrolyte hydrogels.

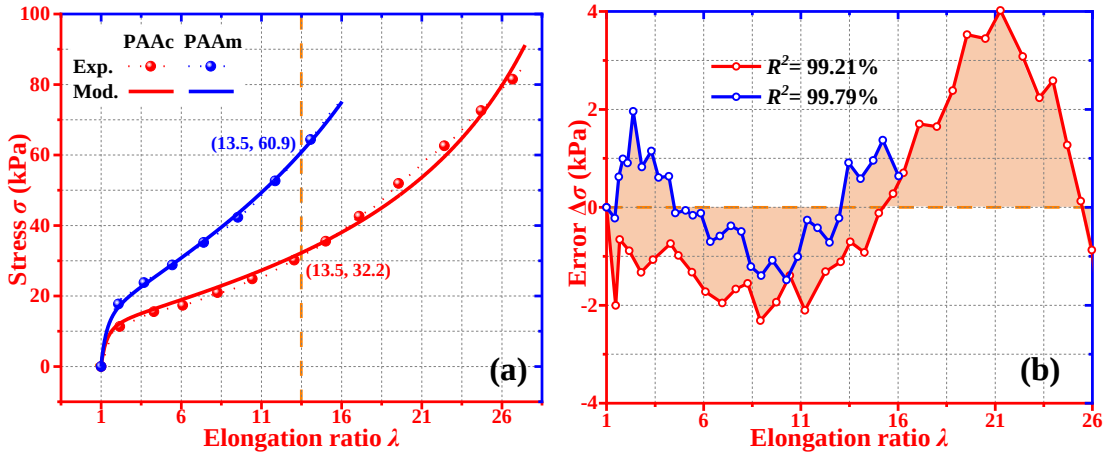

Figure 6. Comparisons of analytical results using equation (11) and experimental data [40] of the stress as a function of elongation ratio for PAAc and PAAm polyelectrolyte hydrogels. (a) The stress-elongation ratio curves. (b) Divergences of analytical and experimental results of stress.

To verify the proposed model using equation (11), the obtained analytical results have been plotted in Figure 7 to predict the stress-elongation ratio behavior of the P(VBIM$^+$-co-v-lignin-co-AM) (VBIM$^+$: 1-vinyl-3-butylimidazolium bromide, v: vinyl, AM: acrylamide) polyelectrolyte hydrogel [41]. All the parameters used in the calculation using equation (11) are listed in Table 3. The experimental data [41] and the analytical results based on the classical Gent model [36,37] are plotted in Figure 7 for comparisons. With an increase in the VBIM$^+$ concentration from 6%, 8%, 10%, 12% to 14%, the stress of molecular network is gradually decreased from 80.2 kPa, 65.6 kPa, 46.7 kPa, 41.0 kPa to 18.2 kPa at the same elongation ratio of λ=7, as shown in Figure 7(a). Figure 7(b) shows the correlation index R^2 between the analytical and

experimental results, which are 94.33%, 98.56%, 99.00%, 99.61% and 96.03% for $VBIM^+$ concentration of 6%, 8%, 10%, 12% and 14%, respectively. It can be clearly seen that the analytical results obtained using equation (11) agree well with the experimental data ($|\Delta\sigma|$<15 kPa).

Table 3. Values of parameters used in equation (11) for P($VBIM^+$-co-v-lignin-co-AM) polyelectrolyte hydrogels.

$VBIM^+$	$N_e k_B T$(kPa)	N	d	J_m	$\frac{h_s^2 \lambda}{2b^2 \xi}$
6%	4.02	76			
8%	3.39	75			
10%	2.39	74	4	430	0.1
12%	3.82	31			
14%	1.75	24			

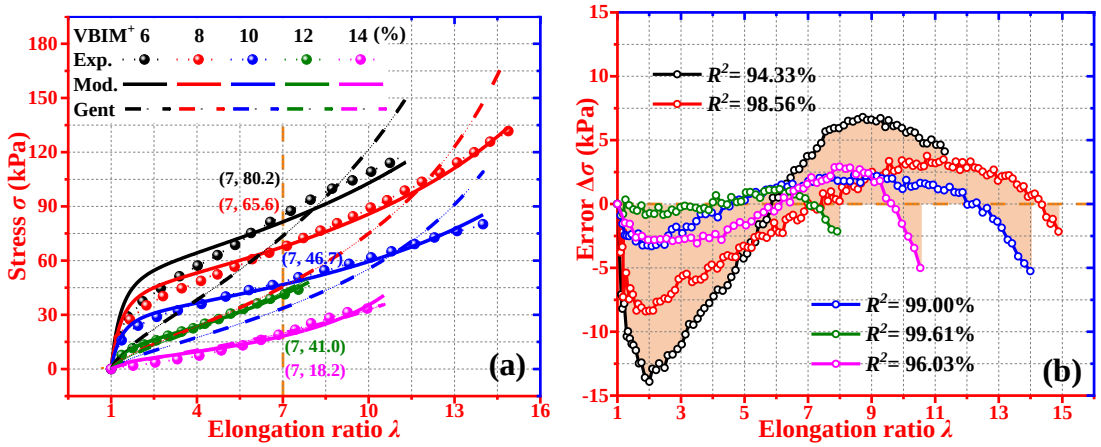

Figure 7. Comparisons among analytical results using equation (11), using the classical Gent model [36,37], and experimental data [41] of the stress as a function of elongation ratio for P($VBIM^+$-co-v-lignin-co-AM) polyelectrolyte hydrogels. (a) The stress-elongation ratio curves. (b) Divergences of analytical and experimental results of stress.

Figure 8(a) plots the theoretically obtained stress-elongation ratio values and experimentally obtained ones for polyelectrolyte hydrogels of P(NaSS-co-DMAEA-Q-co-UM) (NaSS: sodium *p*-styrenesulfonate, DMAEA-Q: dimethylaminoethylacrylate quaternized ammonium, UM: 2-ureidoethyl methacrylate)

with physical crosslinker UM's concentrations of 0.5%, 1%, 2.5% and 10% [42]. All the parameters used in the calculation using equation (11) are listed in Table 4. With an increase in the UM concentration from 0.5%, 1%, 2.5% to 10%, the stress is increased from 33.7 kPa, 50.1 kPa, 57.8 kPa to 150.9 kPa at the same elongation ratio of λ=6. These analytically and experimentally obtained results reveal that the stress of molecular network can be significantly enhanced from 33.7 kPa to 150.9 kPa (an increase of 447%), with an increase in the UM concentration from 0.5% to 10%.

Table 4. Values of parameters used in equation (11) for P(NaSS-co-DMAEA-Q-co-UM) polyelectrolyte hydrogels.

UM	$N_{el}k_BT$(kPa)	N	d	J_m	$\frac{h_s^2\dot{\lambda}}{2b^2\xi}$
0.5%	3.78	29	4	430	0.1
1%	5.42	33			
2.5%	5.98	36			
10%	14.66	37			

Moreover, the correlation index (R^2) between the analytical and experimental results have been calculated, and the obtained results are 99.70%, 99.49%, 99.77% and 96.15% for P(NaSS-co-DMAEA-Q-co-UM) polyelectrolyte hydrogels with the UM concentrations of 0.5%, 1%, 2.5% and 10%, respectively, as shown in Figure 8(b). It can be seen that the analytical results agree well with the experimental data [42], with the divergence of stress being limited to $|\Delta\sigma|$<12.5 kPa. The working principle of physical crosslinker of UM in the P(NaSS-co-DMAEA-Q-co-UM) polyelectrolyte hydrogels is illustrated in Figure 8(c). It is clearly observed that with an increase in UM concentration, both the number of crosslink point (or vertex number (N)) and the functionality of crosslink point (or mean degree (d)) increases,

which is the reason why a stronger polyelectrolyte hydrogel can be obtained.

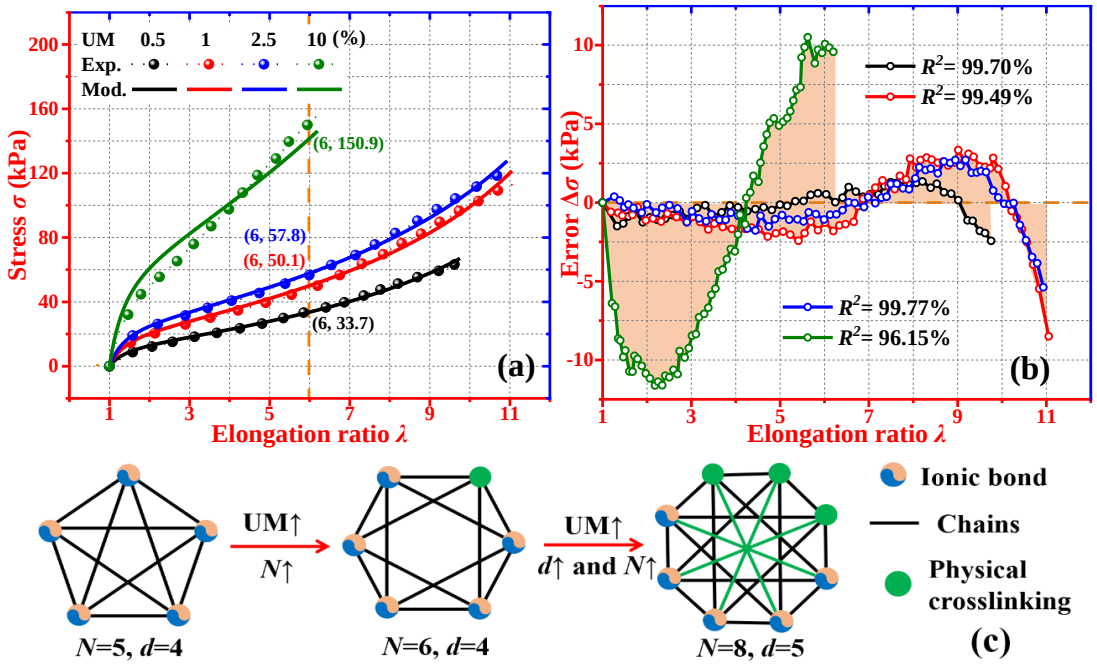

Figure 8. Comparisons of analytical results using equation (11) and experimental data [42] of the stress as a function of elongation ratio for P(NaSS-co-DMAEA-Q-co-UM) polyelectrolyte hydrogels. (a) The stress-elongation ratio curves. (b) Divergences of analytical and experimental results of stress. (c) Schematic illustration of the graph theory, which is determined by the physical crosslinker of UM.

Experimental data [21] for the polyelectrolyte hydrogels of P(NaSS-co-MPTC) (MPTC: 3-(methacryloylamino) propyltrimethylammonium chloride) were compared with the analytical results obtained from equation (11). All the parameters used in the calculation using equation (11) are listed in Table 5. With an increase in the NaCl concentration from 0 mol/L, 0.06 mol/L, 0.15 mol/L to 0.3 mol/L, the stress of P(NaSS-co-MPTC) polyelectrolyte hydrogel is gradually decreased from 2.49 MPa, 1.58 MPa, 0.93 MPa to 0.47 MPa at the same elongation ratio of λ=10, as shown in Figure 9(a). Furthermore, the divergences between the analytical and experimental results [21] of the P(NaSS-co-MPTC) polyelectrolyte hydrogels were calculated using

the correlation index (R^2), and the obtained results are 99.11%, 99.77%, 99.31% and 93.19% for the concentrations of NaCl of 0 mol/L, 0.06 mol/L, 0.15 mol/L and 0.3 mol/L, respectively, as shown in Figure 9(b). These analytical results fit well with the experimental data with errors limited to $|\Delta\sigma|<0.20$ MPa.

Table 5. Values of parameters used in equation (11) for P(NaSS-co-MPTC) polyelectrolyte hydrogels with various NaCl concentrations.

NaCl(mol/L)	$N_{el}k_BT$(kPa)	N	d	J_m	$\frac{h_s^2\lambda}{2b^2\xi}$
0	112	55	4	240	0.07
0.06	71	50			
0.15	41	45			
0.3	20	44			

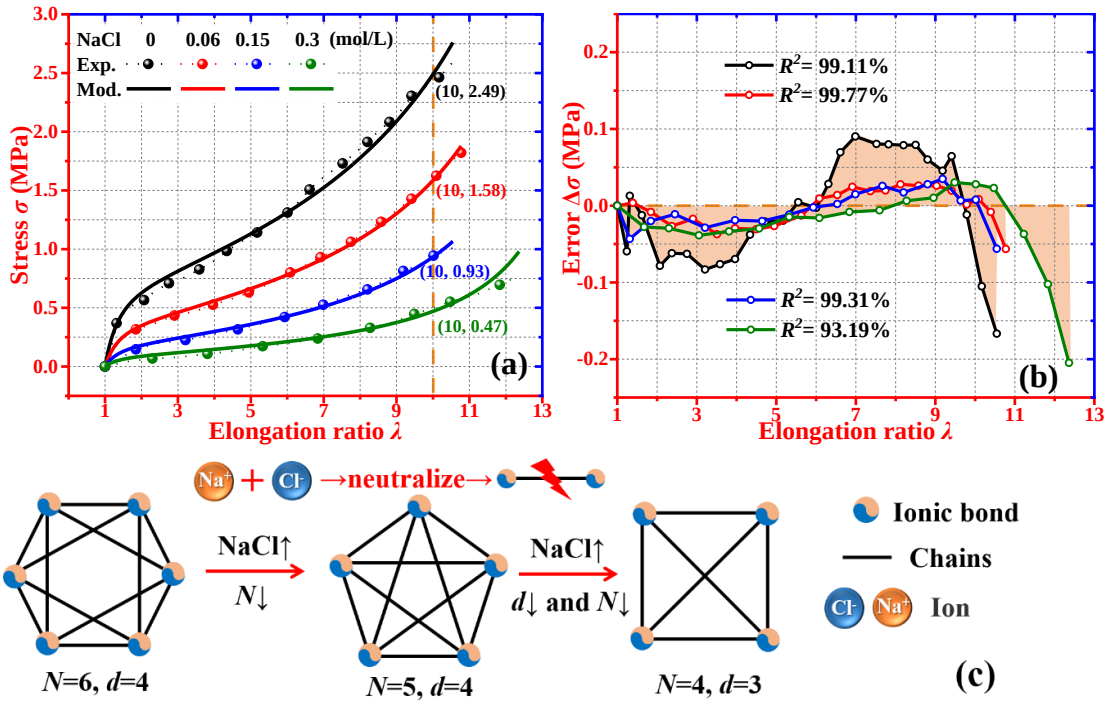

Figure 9. Comparisons of analytical results using equation (11) and experimental data [21] of the stress as a function of elongation ratio for P(NaSS-co-MPTC) polyelectrolyte hydrogels. (a) The stress-elongation ratio curves. (b) Divergences of analytical and experimental results of stress. (c) Schematic illustration of the graph network, which is determined by the NaCl concentration.

The working principle of NaCl concentration in the P(NaSS-co-MPTC)

polyelectrolyte hydrogel is illustrated in Figure 9(c). With an increase in NaCl concentration, both the number of crosslink points (or vertex number (N)) and the functionality of crosslink point (or mean degree (d)) are decreased, resulting into a lower stress of the polyelectrolyte hydrogel.

To verify the proposed model and quantitatively study the effect of monomer concentrations (C_m) of gel on mechanical behaviors, a group of experimental data of P(NaSS-co-MPTC) polyelectrolyte hydrogels reported in Ref. [21] were employed to compare with the analytical results using equation (11). The analytical results of stress values as a function of elongation ratio are plotted in Figure 10. The parameters used in equation (11) are listed in Table 6. As revealed by both the experimental and analytical results, the stress is gradually increased from 0.54 MPa, 0.84 MPa, 1.01 MPa to 1.03 MPa, with an increase in the monomer concentrations (C_m) of P(NaSS-co-MPTC) polyelectrolyte gel from 1.5 mol/L, 1.75 mol/L, 2 mol/L to 2.1 mol/L, at the same elongation ratio of λ=5. It can be clearly seen that these analytical results agree well with the experimental data. Meanwhile, the correlation index (R^2) between the analytical and experimental results were obtained as 96.54%, 97.08%, 98.59% and 98.46% for the polyelectrolyte hydrogels with the gel monomer concentrations (C_m) of 1.5 mol/L, 1.75 mol/L, 2 mol/L and 2.1 mol/L, respectively, as shown in Figure 10(b). The working principle of monomer concentration (C_m) in the P(NaSS-co-MPTC) polyelectrolyte hydrogel is illustrated in Figure 10(c). Based on the bead-spring model [26] and rubber elastic theory [39], the mechanical strength can be improved with an increase in the mean degree (d), which is able to increase the

end-to-end distance (h) resulted from involvements of a large number of molecules in the network per volume to resist the external mechanical loading.

Table 6. Values of parameters used in equation (11) for P(NaSS-co-MPTC) polyelectrolyte hydrogels with different monomer concentrations of gel.

C_m(mol/L)	$N_{el}k_BT$(kPa)	d	N	J_m	$\frac{h_s^2\dot{\lambda}}{2b^2\xi}$
1.5	40	2	50	230	0.07
1.75	77	3			
2	106	4			
2.1	118	5			

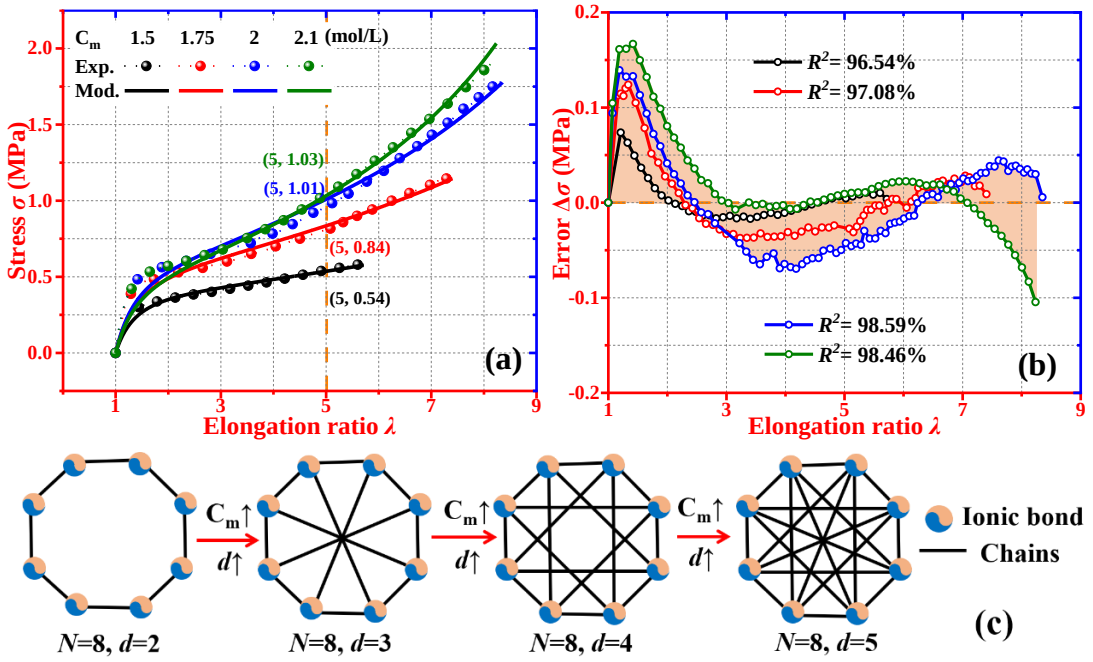

Figure 10. Analytical results and experimental data [21] of stress-elongation ratio curves of P(NaSS-co-MPTC) polyelectrolyte hydrogels, with monomer concentration (C_m) of gel of 1.5 mol/L, 1.75 mol/L, 2 mol/L and 2.1 mol/L. (a) The stress-elongation ratio curves. (b) Divergences of analytical and experimental results of stress. (c) Schematic illustration of the graph network, which is determined by the monomer concentration (C_m) of gel.

4. Conclusions

In this study, a graph theory framework is established to understand the coupling between crosslink points/vertices and chains/edges in the molecular networks, of

which the dynamic elasticity is explored for the polyelectrolyte hydrogels. The adjacency matrix (**A**) parameters, eigenvalue (Λ_i), number of vertex (N) and mean degree (d_i), are applied to estimate the dynamic elasticity of graphical networks. This graphical model is able to combine with the topological parameters (e.g., N and d_i) and dynamic elasticity, to explore the working principle of vertices and edges in the elasticity of molecular network. Furthermore, a constitutive stress-strain relationship is formulated based on the bead-spring model. The obtained analytical results have been verified using both the FEA simulation results and experimentally obtained data reported in literature. Therefore, the proposed model provides a novel fundamental approach to explore the working principle of graph theory for the dynamic elasticity of the molecular network.

Acknowledgements

This work was financially supported by the National Natural Science Foundation of China (NSFC) under Grant No. 11725208 and 12172107, International Exchange Grant (IEC/NSFC/201078) through Royal Society UK and the NSFC.

References

[1] Vatankhah-Varnosfaderani M, Keith A N, Cong Y, Liang H, Rosenthal M, Sztucki M, Clair C, Magonov S, Ivanov D A, Dobrynin A V and Sheiko S S 2018 Chameleon-Like Elastomers with Molecularly Encoded Strain-Adaptive Stiffening and Coloration *Science* **359** 1509-1513

[2] Zhu P, Chen R, Zhou C, Aizenberg M, Aizenberg J and Wang L 2021 Bioinspired Soft Microactuators *Adv. Mater.* **33** 2008558

[3] Zhao Z, Wang H, Shang L, Yu Y, Fu F, Zhao Y and Gu Z 2017 Bioinspired Heterogeneous Structural Color Stripes from Capillaries *Adv. Mater.* **29** 1704569

[4] Forterre Y and Dumais J 2011 Generating Helices in Nature *Science* **333** 1715-1716

[5] Forterre Y, Skotheim J M, Dumais J and Mahadevan L 2005 How the Venus Flytrap Snaps *Nature* **433** 421-425

[6] Sun B, Jia R, Yang H, Chen X, Tan K, Deng Q and Tang J 2022 Magnetic Arthropod Millirobots Fabricated by 3D-Printed Hydrogels *Adv. Intell. Syst.* **4** 2100139

[7] Dumais J and Forterre Y 2012 "Vegetable Dynamicks": The Role of Water in Plant Movements *Annu. Rev. Fluid Mech.* **44** 453-478

[8] Liu X, Gao M, Chen J, Guo S, Zhu W, Bai L, Zhai W, Du H, Wu H, Yan C, Shi Y, Gu J, Qi H J and Zhou K 2022 Recent Advances in Stimuli-Responsive Shape-Morphing Hydrogels *Adv. Funct. Mater.* 2203323

[9] Daly A C, Riley L, Segura T and Burdick J A 2020 Hydrogel Microparticles for Biomedical Applications *Nat. Rev. Mater.* **5** 20

[10] Meyers M A, McKittrick J and Chen P-Y 2013 Structural Biological Materials: Critical Mechanics-Materials Connections *Science* **339** 773-779

[11] Meyers M A, Chen P-Y, Lin A Y-M and Seki Y Biological Materials: Structure and Mechanical Properties *Prog. Mater. Sci.* **53** 1-206

[12] de Gennes P G 1992 Soft Matter *Reviews of Modern Physics* **64** 645-648

[13] Sun J Y, Zhao X, Illeperuma W R K, Chaudhuri O, Oh K H, Mooney D J, Vlassak J J and Suo Z 2012 Highly Stretchable and Tough Hydrogels *Nature* **489** 133-136

[14] He P, He J, Huo Z and Li D 2022 Microfluidics-Based Fabrication of Flexible Ionic Hydrogel Batteries Inspired by Electric Eels *Energy Storage Materials* **49** 348-359

[15] Zhou Y, Wan C, Yang Y, Yang H, Wang S, Dai Z, Ji K, Jiang H, Chen X and Long Y 2019 Highly Stretchable, Elastic, and Ionic Conductive Hydrogel for Artificial Soft Electronics *Adv. Funct. Mater.* **29** 1806220

[16] Yin M J, Yao M, Gao S, Zhang A P, Tam H Y and Wai P K A 2016 Rapid 3D Patterning of Poly(Acrylic Acid) Ionic Hydrogel for Miniature pH Sensors *Adv. Mater.* **28** 1394-1399

[17] Zhao S, Tseng P, Grasman J, Wang Y, Li W, Napier B, Yavuz B, Chen Y, Howell L, Rincon J, Omenetto F G and Kaplan D L 2018 Programmable Hydrogel Ionic Circuits for Biologically Matched Electronic Interfaces *Adv. Mater.* **30** 1800598

[18] Patil V P, Sandt J D, Kolle M and Dunkel J 2020 Topological Mechanics of Knots and Tangles, Science **367** 71-75

[19] Yang S, Tao X, Chen W, Mao J, Luo H, Lin S, Zhang L and Hao J 2018 Mechanics of Self-Healing Polymer Networks Crosslinked by Dynamic Bonds *J. Mech. Phys. Solids* **121** 409-431

[20] Sun T L, Luo F, Kurokawa T, Karobi S N, Nakajima T and Gong J P 2015 Molecular Structure of Self-Healing Polyampholyte Hydrogels Analyzed from Tensile Behaviors *Soft Matter* **11** 9355-9366

[21] Sun T L, Kurokawa T, Kuroda S, Ihsan A B, Akasaki T, Sato K, Haque M A, Nakajima T and Gong J P 2013 Physical Hydrogels Composed of Polyampholytes Demonstrate High Toughness and Viscoelasticity *Nat. Mater.* **12** 932-937

[22] Xiang Y H, Zhong D M, Wang P, Yin T H, Zhou H F, Yu H H, Baliga C, Qu S X and Yang W 2019 A Physically Based Visco-Hyperelastic Constitutive Model for Soft Materials *J. Mech. Phys. Solids* **128** 208-218

[23] Xiang Y H, Zhong D M, Wang P, Mao G Y, Yu H H, Qu S X 2018 A General Constitutive Model of Soft Elastomers *J. Mech. Phys. Solids* **117** 110-122

[24] Xing Z Y, Lu H B, Sun A S, Fu Y Q, Shahzad M W and Xu B B 2021 Understanding Complex Dynamics of Interfacial Reconstruction in Polyampholyte Hydrogels Undergoing Mechano-Chemo-Electrotaxis Coupling. *J. Phys. D: Appl. Phys.* **54** 085301

[25] Xing Z Y, Li Z H, Lu H B and Fu Y Q 2021 Self-Assembled Topological Transition via Intra- and Inter-Chain Coupled Binding in Physical Hydrogel Towards Mechanical Toughening *Polymer* **235** 124268

[26] Rouse P E 1953 A Theory of the Linear Viscoelastic Properties of Dilute Solutions of Coiling Polymers *J. Chem. Phys.* **21** 1272-1280

[27] Yang Y 1998 Graph Theory of Viscoelastic and Configurational Properties of Gaussian Chains *Macromol. Theory Simul.* **7** 521-549

[28] Garcia-Domenech R, Galvez J, de Julian-Ortiz J V and Pogliani L 2008 Some New Trends in Chemical Graph Theory *Chem. Rev.* **108** 1127-1169

[29] Amigó J M, Gálvez J and Villar V M 2009 A Review on Molecular Topology: Applying Graph Theory to Drug Discovery and Design *Naturwissenschaften* **96** 749-761

[30] Bicerano J 1996 Prediction of the Properties of Polymers from Their Structures *Journal of Macromolecular Science, Part C: Polymer Reviews* **C36** 161-196

[31] Chompff A J 1970 Normal Modes of Branched Polymers. I. Simple Ring and Star-Shaped Molecules *J. Chem. Phys.* **53** 1566-1576

[32] Eichinger B E and Martin J E 1978 Distribution Functions for Gaussian Molecules. II. Reduction of the Kirchhoff matrix for Large Molecules *J. Chem. Phys.* **69** 4595-4599

[33] Choi J-H, Lee H, Choi H R and Cho M 2018 Graph Theory and Ion and Molecular Aggregation in Aqueous Solutions *Annu. Rev. Phys. Chem.* **69** 125-149

[34] White A T 1994 An Introduction to Random Topological Graph Theory *Combinatorics, Probability and Computing* **3** 545-555

[35] Watts D J and Strogatz S H 1998 Collective Dynamics of "Small-World" Networks *Nature* **393** 440-442

[36] Gent A N 1996 A New Constitutive Relation for Rubber *Rubber Chem.Technol.* **69** 59-61

[37] Horgan C O, Saccomandi G 2003 Finite Thermoelasticity with Limiting Chain Extensibility *J. Mech. Phys. Solids* **51** 1127-1146

[38] Fried J R 2014 Polymer Science and Technology. United States of America: Pearson Education Press

[39] Treloar L R G 1975 The Physics of Rubber Elasticity. New York: Oxford University

[40] Gulyuz U and Okay O 2013 Self-Healing Polyacrylic Acid Hydrogels *Soft Matter* **9** 10287

[41] Qu X, Zhao Y, Chen Z, Wang S, Ren Y, Wang Q, Shao J, Wang W and Dong X 2021 Thermoresponsive Lignin-Reinforced Poly(Ionic Liquid) Hydrogel Wireless Strain Sensor *Research* **2021** 9845482

[42] Wu S, Shao Z, Xie H, Xiang T and Zhou S 2021 Salt-Mediated Triple Shape-Memory Ionic Conductive Polyampholyte Hydrogel for Wearable Flexible Electronics *J. Mater. Chem. A* **9** 1048-1061